

Neuroradiological findings in *GAA-FGF14* ataxia (SCA27B): more than cerebellar atrophy.

Shihan Chen¹, Catherine Ashton^{1,2}, Rawan Sakalla¹, Guillemette Clement³, Sophie Planel³, Céline Bonnet³, Phillipa Lamont², Karthik Kulanthaivelu⁴, Atchayaram Nalini⁵, Henry Houlden⁶, Antoine Duquette⁷, Marie-Josée Dicaire¹, Pablo Iruzubieta Agudo⁸, Javier Ruiz Martinez⁸, Enrique Marco de Lucas⁹, Rodrigo Sutil Berjon⁹, Jon Infante Ceberio¹⁰, Elisabetta Indelicato¹¹, Sylvia Boesch¹¹, Matthis Synofzik^{12,13}, Benjamin Bender¹⁴, Matt C. Danzi¹⁵, Stephan Zuchner¹⁵, David Pellerin^{1,6}, Bernard Brais^{1,16} Mathilde Renaud³, and Roberta La Piana^{1,16,17}

Affiliations

¹Department of Neurology and Neurosurgery, Montreal Neurological Institute, McGill University, Montreal, QC, Canada

²Department of Neurology, Royal Perth Hospital, Perth, Western Australia

³Service de Neurologie, CHRU de Nancy, France

⁴Department of Neuro Imaging and Interventional Radiology, National Institute of Mental Health and Neurosciences, Bengaluru, India

⁵Department of Neurology, National Institute of Mental Health and Neurosciences, Bengaluru, India

⁶Department of Neuromuscular Disease, UCL Queen Square Institute of Neurology and The National Hospital for Neurology and Neurosurgery, University College London, London, UK

⁷Department of Neurosciences, Faculty of Medicine, Université de Montréal; Centre de Recherche du Centre Hospitalier de l'Université de Montréal (CRCHUM), Montreal, QC, Canada

⁸Department of Neurology, University Hospital of Donostia, Biogipuzkoa Health Research Institute, San Sebastian, Spain

⁹Department of Radiology, University of Cantabria, Spain

¹⁰Department of Medicine and Psychiatry, University of Cantabria, Spain

¹¹Department of Neurology, Medical University of Innsbruck, Austria

¹²Division Translational Genomics of Neurodegenerative Diseases, Center for Neurology and Hertie-Institute for Clinical Brain Research, University of Tübingen, Germany

¹³German Center for Neurodegenerative Diseases (DZNE), Tübingen, Germany

¹⁴Department of Diagnostic and Interventional Neuroradiology, University of Tübingen, Germany

¹⁵Department of Human Genetics, University of Miami Miller School of Medicine, Miami, FL, USA

¹⁶The Neuro (Montreal Neurological Institute-Hospital), McGill University

¹⁷Department of Diagnostic Radiology, McGill University, Montreal, QC, Canada

Corresponding Author

Roberta La Piana

Department of Neurology & Neurosurgery and Department of Diagnostic Radiology

Montreal Neurological Institute and Hospital, McGill University

3801 rue University, Montreal, Quebec, Canada H3A 2B4

roberta.lapiana@mcgill.ca

Abstract

Background

GAA-*FGF14* ataxia (SCA27B) is a recently reported late-onset ataxia caused by a GAA repeat expansion in intron 1 of the *FGF14* gene. Initial studies revealed cerebellar atrophy in 74-97% of patients. A more detailed brain imaging characterization of GAA-*FGF14* ataxia is now needed to provide supportive diagnostic features and earlier disease recognition.

Methods

We performed a retrospective review of the brain MRIs of 35 patients (median age at MRI 63 years; range 28-88 years) from Quebec (n=27), Nancy (n=3), Perth (n=3) and Bengaluru (n=2) to assess the presence of atrophy in vermis, cerebellar hemispheres, brainstem, cerebral hemispheres, and corpus callosum, as well as white matter involvement. Following the identification of the superior cerebellar peduncles (SCPs) involvement, we verified its presence in 54 GAA-*FGF14* ataxia patients from four independent cohorts (Tübingen n=29; Donostia n=12; Innsbruck n=7; Cantabria n=6). To assess lobular atrophy, we performed quantitative cerebellar segmentation in 5 affected subjects with available 3D T1-weighted images and matched controls.

Results

Cerebellar atrophy was documented in 33 subjects (94.3%). We observed SCP involvement in 22 subjects (62.8%) and confirmed this finding in 30/54 (55.6%) subjects from the validation cohorts. Cerebellar segmentation showed reduced mean volumes of lobules X and IV in the 5 affected individuals.

Conclusions

Cerebellar atrophy is a key feature of GAA-*FGF14* ataxia. The frequent SCP involvement observed in different cohorts may facilitate the diagnosis. The predominant involvement of lobule X correlates with the frequently observed downbeat nystagmus.

Introduction

Late-onset cerebellar ataxias (LOCA), defined by the onset of progressive cerebellar syndrome after 30 years of age, are heterogenous neurodegenerative disorders that have largely resisted molecular diagnosis until recently.^{1, 2} GAA-*FGF14* ataxia (spinocerebellar ataxia SCA27B; OMIM 620174) is a recently described LOCA caused by a dominantly inherited GAA-TCC repeat expansion in the first intron of *FGF14*, which encodes the fibroblast growth factor-14.^{3, 4} This disorder is estimated to be one of the most common forms of late-onset as well as autosomal dominant ataxias, especially in the French Canadian (around 60% of previously undiagnosed patients with LOCA) and European population (around 20% of all autosomal dominant ataxias).⁵ Initial review of brain MRI findings has revealed cerebellar atrophy in 74% of GAA-*FGF14* ataxia patients, with further data reporting vermian atrophy in over 90% of patients.^{3, 6} It is now important to precisely define the neuroradiological features of GAA-*FGF14* ataxia that distinguish it from other LOCAs, to 1) provide supportive diagnostic features to ensure early diagnosis, and 2) explore its pathophysiological bases.

Methods

We performed a retrospective analysis of MRI images of patients with GAA-*FGF14* ataxia. Subjects were included if a) their phenotype was clinically compatible with GAA-*FGF14* ataxia, b) the genetic testing documented a (GAA)_{≥250} expansion in *FGF14*, according to Bonnet et al.,⁷ and c) available MRI scans included at least sagittal or 3D T1- or 3D FLAIR (Fluid-attenuated inversion recovery) T2-weighted images.^{7, 8} Subjects were recruited in Quebec (n=27), Nancy (n=3), Perth (n=3) and Bengaluru (n=2). For all subjects, we collected demographic and clinical data.

All images were reviewed collegially by the authors (SC, RS, CA, and RLP) according to the qualitative approach detailed below and blind to disease severity and presented symptoms. Each MRI scan was evaluated twice, 3 months apart. Team disagreements were resolved by consensus. The institutional review boards of each participating institution approved the use of clinical data for the retrospective study.

Qualitative MRI analysis

We performed a qualitative analysis to assess the degree of atrophy in the vermis, cerebellar hemispheres, and cerebral hemispheres (size of ventricular system and CSF spaces). For the vermis the atrophy was assessed on midline sagittal planes as ‘present’ or ‘absent’, with further grading as ‘mild’, ‘moderate’ or ‘severe’. For the cerebellar and cerebral hemispheres, the atrophy was assessed on all planes and, when present, graded as ‘mild’, ‘moderate’ or ‘severe’. The effect of the patient’s age was taken into consideration by comparing the images to standard image series used in a study of a neurologically healthy population.⁹

To assess the presence of brainstem atrophy we measured the maximal anteroposterior diameter at the level of the midbrain, midpons, and medulla on sagittal images, and compared to normative values for age according to Metwally et al.¹⁰ The corpus callosum thickness was quantified by measuring the maximum width of the body at midpoint and compared to normative values according to Gupta et al.¹¹

We also assessed the presence and characteristics of white matter abnormalities on T2- and FLAIR T2-weighted images on all planes, when available, by location (periventricular, subcortical, juxtacortical), lobar involvement (frontal, parietal, temporal, occipital, cerebellar, brainstem), and symmetry. Juxtacortical lesions were defined as lesions in direct contact with the cortical ribbon. Periventricular lesions included all lesions abutting any portion of lateral

ventricles. Subcortical lesions were defined as supratentorial non-juxtacortical and non-periventricular. As for the assessment of atrophy described above, the effect of the patient's age was taken into consideration by comparing to standard images and prevalence across age from previous studies of healthy subjects.^{9, 12}

The protocols of the reviewed MRIs were not standardized, as they were requested for clinical indication across different hospitals and scanners, thus limiting the systematic analysis of MR data.

Clinical-radiological correlations

We compared the prevalence of radiological findings (cerebral, cerebellar and vermian atrophy; superior cerebellar peduncle (SCP) involvement, periventricular and multifocal white matter abnormalities; corpus callosum thinning; ventricular enlargement) between patients symptomatic for \leq vs. $>$ than 5 years ($n=11$ and $n=24$, respectively) at the time of initial MRI scan, since most patients become permanently ataxic after an average of 5 years since disease onset, and between patients aged \leq vs $>$ 60 years-old ($n=14$ and $n=21$ respectively) at the time of their initial MRI. We assessed differences between groups with the Fisher's exact test. Additionally, we sought to compare the radiological findings between subjects with episodic ataxia vs. permanent ataxia at the time of MRI, and between subjects with GAA expansion size <300 vs. ≥ 300 . However, the highly unequal sample size between groups prevented optimal statistical testing. Results from all analyses are included in the supplementary material (**Supplementary Table 3**).

Secondary Analysis

Following the identification of the involvement of the SCPs, we sought to verify its presence in four independent cohorts from Tübingen (Germany), Innsbruck (Austria), Santander (Spain), and

San Sebastian (Spain). Neurologists and radiologists from each center (M.S. and B.Be., University of Tübingen; E.I., S. B. University of Innsbruck; P.I.A, A.L.M.A., University of Donostia; J.I.C., E.M.L., R.S.B. University of Cantabria) reviewed the brain MR images of their *GAA-FGF14* ataxia patients (Tübingen n=31; Donostia n=14; Innsbruck n=9; Cantabria n=6) to assess the presence of the SCP involvement comparing to provided reference images (**Supplementary Figure 1**). The Montreal group also independently reviewed the same MRIs, blind to the treating teams' conclusions. Disagreement between the two assessments were solved by consensus.

Measurements and Quantitative MRI analysis

To assess the degree of cerebellar atrophy, we performed quantitative MRI analyses on individuals with confirmed *GAA-FGF14* ataxia and available 3D T1-weighted images. Five subjects of the entire cohort (5/35; 14.3%) fulfilled the required imaging criteria. We also performed the quantitative MRI analysis on 5 age-matched healthy controls with available 3D T1-weighted images.

Segmentation of cerebellum using T1-weighted images was performed automatically using the CERES pipeline (volBrain)¹³ (**Supplementary Figure 2**). All anatomical structures were defined based on the MRI atlases described in Park et al., 2014.¹⁴ We compared the following parameters between affected individuals and controls: total and lobular cerebellum volume (grey matter and white matter), cerebellar cortical thickness, and asymmetry index. Cerebellar volume percentage was calculated as the ratio between cerebellar volume and total intracranial volume.

Results

We reviewed brain MRI studies of 35 patients (14 not previously reported): 15 females, median age at MRI was 63 years (range 28-88 years); median disease duration at the time of MRI was 9 years (range 1-34 years), median age of disease onset at 52 years (range 25-75 years). The clinical and radiological features of the cohort are summarized in **Table 1**. Longitudinal studies were also available for seven subjects. In terms of disease duration, 24 patients (54.3%) were symptomatic for >5 years at the time of initial MRI.

Radiological Features

MRI patterns of atrophy

Infratentorial atrophy

Cerebellar atrophy was observed in 33 patients (33/35, 94.3%), including 22 patients (22/35, 62.8%) with involvement of both vermis and cerebellar hemispheres, and 11 (11/35, 31.4%) with isolated vermian atrophy (**Figure 1**).

For the 33 patients with vermian atrophy – either isolated or not – the degree was mild in 13 (13/35, 37.1%), moderate in 17 (17/35, 48.5%), and severe in 3 (3/35, 8.5%). The majority of patients (32/35, 91.4%) had predominant involvement of the anterior lobe and the superior posterior lobe of the vermis before the pre-pyramidal fissure, except for one individual with diffuse atrophy involving the vermis globally.

Among the 22 patients with both vermian and hemispheric involvement, cerebellar hemispheres were mildly atrophic in 15 subjects (15/35, 42.8%), moderately atrophic in six (6/35, 17.1%), and severely atrophic in one (1/35, 2.9%). The degree of atrophy was the same in both the vermis and cerebellar hemispheres in 11 (50%), relatively more severe in the vermis compared to the

hemispheres in ten (10/22, 45.5%) and more severe in the cerebellar hemispheres in one patient (4.5%).

We documented reduced brainstem anteroposterior diameter in one subject (1/35; 2.8%) (AP diameter 1.77mm, normal range for age 1.9-2.5) who presented concomitant vermian and cerebellar hemispheric atrophy as well as SCP involvement.

Supratentorial atrophy

Cerebral atrophy was present in 15 subjects (15/35, 42.9%; median age 69 years, range 45-80): mild in 11 (11/35, 31.4%; median age 63 years, range 45-80), and moderate in four (4/35, 11.4%; median age 73 years, range 67-77). This was particularly evident in terms of increased CSF spaces in the frontal lobes.

Ventricular enlargement was documented in 13 subjects (13/35, 37.1%); limited to the 4th ventricle in four (4/35, 11.4%) and extended to the lateral ventricles in 9 (9/35, 25.7%).

We documented reduced corpus callosum body thickness for age in 7 subjects (7/35; 20%): (0.32, 0.35, 0.38, 0.39, 0.44, 0.48, 0.48mm; mean value for age 0.65 ± 0.15).

Longitudinal studies

The mean interval between MRIs was 6.4 years (range 1-16 years). All seven patients had cerebellar atrophy on the initial MRI, which remained stable in two patients and progressed in five (5/7, 71.4%) (**Figure 2**). We also observed progression of cerebral atrophy in one patient, likely related to age (1/7, 14.3%; age at MRI 63 and 79 years) (**Figure 2D**) and progression of ventricular enlargement in two (2/7, 28.6%). Two patients (2/7, 28.6%) developed corpus callosum thinning on subsequent MRI (**Figure 2D**).

MRI patterns of white matter abnormality

T2 or FLAIR T2-weighted images on all three planes were available for 19 subjects, while for the remaining 16 only axial T2 or FLAIR T2 images were available for review.

White matter abnormalities (WMAs) were present in 34 subjects (34/35, 97.1%; median age 63, range 28-88). Different patterns were observed: a characteristic SCP involvement (**Figure 3**), as well as non-specific periventricular and multifocal abnormalities (**Figure 4**).

SCP involvement

We observed involvement of the SCP and their decussation within the midbrain (**Figure 3**) in 22 subjects (22/35, 62.8%), 16 (16/22, 72.7%) of which had prominent hyperintensity (**Figure 3A-D, I-L**), while six (6/22, 27.2%) presented with more faint changes (**Figure 3E-H**). SCP changes were best captured by 3D FLAIR T2 images and prominent hyperintensity was visible in all three planes (coronal, sagittal, and axial), when available.

SCP involvement in validation cohorts

From the 60 subjects with confirmed *GAA-FGF14* ataxia from the four independent cohorts, we reviewed T2-weighted and FLAIR T2-weighted images of 54 subjects (Tübingen = 29; Donostia = 12; Innsbruck = 7; Cantabria = 6). Six subjects were excluded for poor image quality.

Involvement of the SCP was identified in 30 subjects (30/54, 55.6%). Fifteen of them (15/30; 50%) had prominent T2 or FLAIR T2 hyperintense signal along the SCP, while 15 (15/30; 50%) had faint signal change. **Supplementary Table 1** includes the results for each independent cohort.

Non-specific periventricular and multifocal WMA

Periventricular WMAs were present in 28 (28/35, 80%; median age 64, range 28-88) cases: in six (6/35, 17.1%) they were limited to the white matter adjacent to the anterior horns of the

lateral ventricles, in seven to the posterior horns only (7/35, 20%), and in 14 they extended to both anterior and posterior horns (15/35, 42.9%) (**Figure 4C, D**). A minority (6/35, 17.1%) had more diffuse involvement with extension to the peritrigonal area (**Figure 4B**). Non-specific subcortical multifocal lesions were observed in 22 subjects (22/35, 62.8%; median age 64, range 44-88) (**Figure 4A, B, C**). **Supplementary Table 2** includes the prevalence and p values of periventricular and multifocal abnormalities in the total sample and in different age groups as compared to a previously reported healthy cohort.¹² The prevalence of periventricular white matter abnormalities was significantly higher ($p < 0.05$) in subjects with *GAA-FGF14* ataxia when compared to the healthy population cohort.

Most patients (29/35, 82.9%) had more than one type of WMA: 12 presented periventricular, multifocal, and SCP involvement (12/35, 34.3%), seven (7/35, 20%) had periventricular and multifocal lesions, six (6/35, 17.1%) had both SCP involvement and periventricular changes, and the four (4/35, 11.4%) had SCP involvement and multifocal abnormalities.

Vascular risk factors were documented in 19 patients (19/35, 54.3%). Among these, six (6/19, 31.5%) presented with SCP abnormal signal, ten (10/19, 52.6%) with periventricular white matter involvement, ten (10/19, 52.6%) with multifocal lesions, and seven (7/19, 36.8%) with ventricular enlargement. Approximately one third (6/19, 31.5%) presented with both non-specific white matter lesions and ventricular enlargement.

Longitudinal studies

Among the seven patients with longitudinal MRI studies, SCP involvement was observed on the initial scan in five (5/7, 71.4%), and remained stable overtime. One case showed new onset mild SCP involvement 4 years after the initial MRI study. Progression of periventricular and

multifocal white matter abnormalities was noted in one (1/7, 14.3%) and four (4/7, 57.1%) patients, respectively.

Clinical-radiological correlations

We did not document any statistically significant differences in the presence of neuroradiological findings between patients with \leq vs. $>$ 5 years of disease duration. Cerebral atrophy and ventricular enlargement were more prevalent in older patients (>60 years-old at initial MRI) compared to the rest of the cohort ($p=0.046$; $p=0.033$, respectively). Conversely, isolated vermian atrophy and involvement of the SCP were more prevalent in younger patients (≤ 60 years-old at MRI) ($p=0.023$ and $p<0.001$, respectively). All the p values relative to the comparison between groups are reported in **Supplementary Table 3**.

Quantitative analysis of cerebellar atrophy

Cerebellar Volume

Table 2 includes the results of the quantitative cerebellar volume analysis for the total volume percentage as well as grey matter percentage for the entire cerebellum and individual lobules in the five patients with available 3D T1-weighted images and controls.

We did not observe significant differences in the total cerebellar volume nor total grey matter volume between patients with GAA-*FGF14* ataxia and controls. Analyses of individual lobules revealed a decrease in the total volume percentage of lobule IV (mean $0.24 \pm 0.03\%$ vs $0.31 \pm 0.06\%$, $t(8) = -2.55$, $p=0.017$, 95%CI $[-0.14, -0.007]$) and lobule X (mean $0.07 \pm 0.01\%$ vs $0.1 \pm 0.02\%$, $t(8) = 0.03$, $p=0.008$, 95%CI $[-0.056, -0.007]$) in patients compared to controls. Analysis of grey matter revealed significant decrease in total volume percentage of lobule IV

(mean $0.22 \pm 0.02\%$ vs 0.27 ± 0.06 , $t(8) = -1.99$, $p=0.04$, 95% CI $[-0.11, -0.009]$ and lobule X (mean $0.06 \pm 0.01\%$ vs $0.09 \pm 0.01\%$, $t(8) = -3.17$, $p=0.007$, 95% CI $[-0.046, -0.007]$).

Among all lobes, we observed the greatest total volume percentage difference in lobule X (47.4%). In terms of grey matter volume, lobule X showed the greatest reduction in volume percentage (42.5%).

Discussion

This study confirms that cerebellar atrophy is a common MRI finding in *GAA-FGF14* ataxia and it provides a detailed characterization of it as well as highlights additional neuroradiological features that may facilitate diagnosis.^{3, 6, 15}

Cerebellar atrophy of varying severity was observed in 94% of our subjects, all with vermian involvement, and over half with atrophy extending to the cerebellar hemispheres. Vermian atrophy affected predominantly the anterior lobe and the superior part of the posterior lobe (i.e. declive, folium and tuber lobules). Despite the limited number of available longitudinal MR exams, our study documented progression of cerebellar atrophy in more than half of the subjects with available follow up over a median 6.4-year period, in line with a previous study by Wilke et al.⁶

Cerebellar atrophy is the primary radiological finding in patients with cerebellar ataxia.^{1, 6, 15} In LOCA, cerebellar atrophy has been reported in Spinocerebellar Ataxias (SCA) 8 and 17, *RFC1* related disorder and MSA-C (Multiple System Atrophy-Cerebellar type).¹⁶⁻²² Establishing the pattern of atrophy can guide genetic testing and eventual diagnosis. The preferential involvement of the vermis and, to a lesser degree, cerebellar hemispheres can differentiate *GAA-FGF14* ataxia from other LOCA with more widespread atrophy, but the distinction from other LOCAs

with more isolated involvement of the cerebellum, such as SCA6, can be more challenging.^{18,16}

To attempt to address this, we performed quantitative segmentation of the cerebellum in subjects with available 3D T1-weighted images, which unfortunately were only 14.7% of our cohort, thus limiting the generalizability of our results and needing further confirmation in future prospective studies. In the subjects with GAA-*FGF14* ataxia we assessed, lobules IV and X were preferentially affected, both in total and grey matter volume, with lobule X showing the greatest reduction. Damage to lobule X and flocculus is associated with downbeat nystagmus as hypofunction of lobule X can lead to disinhibition of the superior vestibular nuclei neurons, resulting in spontaneous slow upward drift followed by corrective downward saccade.^{23,24} Gaze-evoked nystagmus is another feature thought to be due to inadequate lobule X control on the brainstem ocular motor integrator.²⁴ These results correspond well with 57% of our cohort having downbeat nystagmus, and 57% having gaze-evoked horizontal nystagmus – rates similar to other reported cohorts (range between 37 and 78%).^{3, 15, 25, 26} Nystagmus was present in all the subjects included in the volumetric analysis. Interestingly, *FGF14* (GAA)_{≥250} expansions were documented in 48% of 170 subjects with ‘idiopathic’ downbeat nystagmus.²⁷ As proposed by Pellerin et al.²⁷, the earliest damage in SCA27B may arise in the flocculus / paraflocculus, thus accounting for the frequently observed early downbeat nystagmus, impaired VOR, other cerebellar ocular motor signs and vertigo. Our data, although preliminary, further support that GAA-*FGF14* ataxia pathology may arise and is particularly severe in this region of the cerebellum. Lobular analysis may aid in the differentiation between LOCAs with similar patterns of global atrophy and should be the focus of future targeted studies. Identification of subregions preferentially affected during the early phase of the disease may promote the development of imaging-markers for early disease detection. As previously found, there is preliminary evidence

that some patients with *GAA-FGF14* disease present symptoms limited to the involvement of the cerebellar flocculus / paraflocculus region and do not develop ataxia even after several years of disease duration.²⁷

Our study is the first to describe the involvement of the SCPs and their decussation within the midbrain in subjects with *GAA-FGF14* ataxia. While microstructural changes and reduced volume have been documented in SCA2 and Friedreich ataxia respectively,³¹⁻³⁴ a pattern of abnormal T2-hypersignal along the SCP like the one we observed in *GAA-FGF14* ataxia subjects has been previously documented in some patients with POLR3-related spastic ataxia.³⁵

³⁶ Co-existent SCP and vermian atrophy was present in 57% of our patients, and could suggest that the SCP abnormality is a reflection of reduced vermis-dentate connectivity secondary to vermian atrophy. SCP changes were best captured by 3D T2 FLAIR images. Given the retrospective nature of our study - which limited the availability of ideal sequences - and the presence of suggestive symptoms in *GAA-FGF14* ataxia, it is reasonable to suspect that SCP involvement may be even more prevalent than what we observed.^{3, 6} Hence, we recommend including 3D FLAIR T2-weighted MR sequence when assessing subjects with suspected SCA27B.

Within the limitations of this study, we did not observe any association between disease duration (less vs. more than 5 years) and neuroradiological findings. Cerebral atrophy and ventricular enlargement were more prevalent in older patients. Since these findings can be part of normal aging process or due to other neurodegenerative processes, it will be important to verify these findings in future case-control prospective studies. More interestingly, SCP involvement and vermian atrophy were more represented in patients younger than 60. While it is expected that cerebellar atrophy may be limited to the vermis in younger patients and then extend to cerebellar

hemispheres over time, the result is more surprising for the SCP involvement. Several confounding factors might have contributed to this. MRIs included in our study have been acquired over a 20-year span of time and the SCP region may not have been well visualised due to outdated MRI sequences and protocols. Additionally, factors such as family history and access to healthcare resources may affect the timing of one's initial MRI scan, thus limiting the assessment of differences between groups. Although we cannot completely exclude that the signal abnormalities along the SCP might be transitory, the fact that we documented it in longitudinal exams argues against it. Only prospective dedicated neuroimaging studies will elucidate the diagnostic value of the SCP signal abnormalities, their association with age or clinical features, and their role in the disease pathophysiology. Although formal statistical analysis was prevented by unequal sample sizes between groups, we observed SCP involvement in subjects with episodic ataxia as well as permanent ataxia, and in subjects with (GAA) repeat expansion size below as well as above 300. Therefore, SCP involvement may be a useful additional diagnostic feature, particularly in patients with an incompletely penetrant (GAA)₂₅₀₋₂₉₉ repeat expansion, in earlier stages of disease when only episodic features are observed, and as a marker distinguishing this disorder from other forms of LOCA.^{37, 38}

In addition to the SCP involvement, we documented non-specific periventricular and multifocal white matter abnormalities in 80% and over 60% of individuals respectively. As compared to the data from a large healthy population study, the presence of periventricular changes was significantly higher in the total of GAA-*FGF14* ataxia subjects, even though we did not observe statistically significant differences when we performed comparison between age subgroups. The small sample size of the subgroups could contribute to the lack of observed differences with the

general population, nonetheless age, cardiovascular risk factors and other neurodegenerative disorders might influence the observed changes.^{6, 39}

In conclusion, we described a novel MRI finding of SCP involvement in *GAA-FGF14* ataxia patients, which may be specific to this LOCA subtype and whose detection can orient and accelerate the diagnosis, especially in the early stages of the disease. Our study confirmed that cerebellar atrophy is a key feature of *GAA-FGF14* ataxia, starting at the level of the vermis and extending to the hemispheres over time. The preferential involvement of lobule X correlates with cerebellar ocular motor signs frequently observed in *GAA-FGF14* patients. Lobular volumetric analysis of *GAA-FGF14* ataxia and further dedicated imaging studies may promote diagnostic accuracy, give insights into disease pathogenesis, and contribute to the development of early disease biomarkers.

Acknowledgements

D. Pellerin has received a fellowship award from the Canadian Institutes of Health Research (CIHR). B. Brais has received funds from the Fondation Groupe Monaco and the Canadian Institutes of Health Research (grant 189963). M.C. Danzi and S. Zuckner were supported by the NIH National Institutes of Neurological Disorders and Stroke (grant 2R01NS072248-11A1 to S.Z.) and the NIH National Human Genome Research Institute (grant R21HG013397).

M.Synofzik and B. Brais were supported by the European Joint Programme on Rare Diseases, as part of the PROSPAX consortium, under the EJP RD COFUND-EJP N° 825575 (DFG, German Research Foundation, No 441409627). R. La Piana has received a Research Scholar Junior 1 award from the Fonds de Recherche du Québec en Santé (FRQS), and research funds from the Canadian Radiological Foundation, Canadian Institutes of Health Research (grant 506913),

Ataxia Canada, the Spastic Paraplegia Foundation and Roche Canada. The authors thank the patients and their families for participating in this study.

Conflicts of Interests

A. Duquette has received consultancy honoraria from AavantiBio, Novartis, Pfizer Canada, PTC Therapeutics, and Reata Pharmaceuticals, all unrelated to the present manuscript. M. Synofzik has received consultancy honoraria from Ionis, UCB, Prevail, Orphazyme, Servier, Reata, GenOrph, AviadoBio, Biohaven, Zevra, Lilly, and Solaxa, all unrelated to the present manuscript. B. Bender is Co-Founder, shareholder and CTO of AIRAmed GmbH. R. La Piana has received speaking honoraria from Novartis unrelated to the present manuscript.

Tables

Table 1. Demographic, clinical and radiological findings of 35 subjects with GAA-FGF14 ataxia. *Legend:* SCP=superior cerebellar peduncle involvement; M = multifocal white matter abnormalities; PB = Periventricular, around anterior and posterior horns; PA = Periventricular, around anterior horns only; PP= Periventricular, around posterior horns only. *Data missing for 4 subjects.

Demographics and clinical information	n (%) - tot 35
Sex F;M	15; 20 (42.8; 57.2)
Median age at onset, years [range]	52 [25-75]
Median age at MRI, years [range]	63 [28-88]
Median disease duration, years [range]	9 [1-34]
Median GAA-TCC repeat expansion [range]	378 [265-508]
Permanent ataxia at time of MRI*	29 (93.5)
Episodic ataxia at time of MRI*	2 (6.5)
Down beat nystagmus	20 (57.1)
Gaze-evoked horizontal nystagmus	20 (57.1)
Vascular risk factors	19 (54.3)
MRI findings	n (%); tot 35
<i>Cerebral atrophy</i>	15 (42.8)
mild	11 (31.4)
moderate	4 (11.4)
<i>Cerebellar involvement</i>	33 (94.3)
<i>Vermian atrophy</i>	33 (94.3)
mild	13 (37.1)
moderate	17 (48.6)
severe	3 (8.6)
<i>Brainstem atrophy</i>	1 (2.8)
<i>Hemispheric atrophy</i>	22 (62.8)
mild	15 (42.8)
moderate	6 (17.1)
severe	1 (2.8)
<i>White matter abnormalities</i>	34 (97.1)
SCP	22 (62.8)
multifocal	22 (62.8)
periventricular	28 (80)
<i>Corpus callosum thinning</i>	7 (20)
<i>Ventricular enlargement</i>	13 (37.1)
4 th ventricle	4 (11)
Extended to lateral ventricles	9 (25.7)

Table 2. Quantitative cerebellar volume analysis in 5 subjects with GAA-*FGF14* ataxia and available high quality sagittal or 3D T1-weighted images and age-matched controls. Mean values, standard deviations, and one-sided p values for the individual lobules for patients (cases) and controls. In bold the statistically significant differences ($p < 0.05$) between groups.

Cerebellar Lobular Total Tissue %

	Mean Cases	St. Dev.	Mean Controls	St. Dev.	one-sided <i>p</i> value
Cerebellum %	7.906	0.506	8.863	1.504	0.18
I-II %	0.006	0.005	0.007	0.002	0.33
III %	0.082	0.026	0.099	0.021	0.14
IV %	0.239	0.029	0.31	0.057	0.02
V %	0.46	0.097	0.59	0.122	0.05
VI %	1.04	0.171	1.26	0.255	0.07
Crus I %	1.67	0.193	1.9	0.33	0.1
Crus II %	1.11	0.037	1.09	0.23	0.43
VIIIB %	0.6	0.106	0.59	0.101	0.41
VIIIA %	0.733	0.087	0.737	0.099	0.47
VIIIB %	0.47	0.101	0.55	0.079	0.11
IX %	0.45	0.067	0.51	0.162	0.24
X %	0.066	0.012	0.098	0.019	0.008

Cerebellar Lobular Grey Matter (%)

	Mean Cases	St. Dev.	Mean Controls	St. Dev.	one-sided <i>p</i> value
Cerebellum %	6.003	0.518	6.664	1.151	0.138
I-II %	0.003	0.003	0.004	0.0005	0.29
III %	0.061	0.011	0.068	0.005	0.14
IV %	0.22	0.023	0.27	0.056	0.04
V %	0.4	0.093	0.5	0.099	0.06
VI %	0.93	0.157	1.14	0.227	0.07
Crus I %	1.37	0.191	1.6	0.306	0.09
Crus II %	0.93	0.024	0.931	0.207	0.49
VIIIB %	0.54	0.037	0.52	0.037	0.38
VIIIA %	0.66	0.086	0.65	0.092	0.44
VIIIB %	0.42	0.095	0.46	0.044	0.39
IX %	0.38	0.042	0.41	0.127	0.33
X %	0.06	0.011	0.09	0.014	0.007

Captions for Figures

Figure 1. Cerebellar atrophy. Sagittal Flair T2 (A, B) and T1-weighted images of three subjects showing different degrees of cerebellar atrophy. A, subject in their 60s with 9 years of disease duration with normal size of vermis (GAA-TCC expansion size 374); B, moderate cerebellar atrophy of the anterior and superior lobe of the vermis in a subject in their 60s with 34 years of disease duration (GAA-TCC expansion size 374); C, severe cerebellar atrophy of the anterior and superior lobe of the vermis in a subject in their 60s with 14 years of disease duration (GAA-TCC expansion size 437).

Figure 2. Cerebellar atrophy, longitudinal data. A,B. Sagittal T1-weighted images of a patient (GAA-TCC expansion size 424) showing stable degree of mild cerebellar atrophy localized mainly in the anterior lobe of the vermis, over the course of 10 years, from their 40s, 17 years after disease onset (A), to their 50s (B). C,D. Sagittal T1-weighted images of a patient showing progression of the vermian atrophy that extended from the anterior lobe of the vermis (C, while in their 60s, 5 years after disease onset) to the posterior aspect of the vermis (D), 16 years after the first MRI. In addition, the images show that the patient developed mild corpus callosum thinning at the level of the body and midline cerebral atrophy over time.

Figure 3. Involvement of the superior cerebellar peduncles. Multiplanar Flair T2-weighted images of three subjects showing bilateral and symmetric involvement of the superior cerebellar peduncles and its decussation within the midbrain. T2-hyperintense signal is visible in the central region of the midbrain both in the axial (A, E, I) and sagittal views (D, H, L), as well as in the coronal plane (C, G, K). The SCPs are involved for their entire length, as showed in the axial views (B, F, J) and in the coronal image (C). The images are from a subject in their 70s with 5 history of disease duration (GAA-TCC expansion size 324) (A-D), a subject in their 80s with 10

years of disease duration (E-H) (GAA-TCC expansion size 250), a subject in their 70s with 21 years of disease duration (GAA-TCC expansion size 357) (I-L).

Figure 4. Non-specific white matter abnormalities. Axial FLAIR T2-weighted images showing different supratentorial white matter abnormalities. A, a focal oval-shaped lesion in the right frontal deep white matter in a subject in their 70s (GAA-TCC expansion size 357); B, multifocal subcortical white matter abnormalities in a subject in their 70s (GAA-TCC expansion size 330); C, symmetric periventricular white matter involvement with enlargement of the lateral ventricles and multifocal subcortical white matter abnormalities in a subject in their 50s (GAA-TCC expansion size 304); D, posterior periventricular white matter involvement in a subject in their 70s (GAA-TCC expansion size 290). None of these subjects were known for vascular risk factors.

References

1. Krygier M, Mazurkiewicz-Beldzinska M. Milestones in genetics of cerebellar ataxias. *Neurogenetics* 2021;22:225-234.
2. Harding AE. "Idiopathic" late onset cerebellar ataxia. A clinical and genetic study of 36 cases. *Journal of the neurological sciences* 1981;51:259-271.
3. Pellerin D, Danzi MC, Wilke C, et al. Deep Intronic FGF14 GAA Repeat Expansion in Late-Onset Cerebellar Ataxia. *The New England journal of medicine* 2023;388:128-141.
4. Rafehi H, Read J, Szmulewicz DJ, et al. An intronic GAA repeat expansion in FGF14 causes the autosomal-dominant adult-onset ataxia SCA50/ATX-FGF14. *American journal of human genetics* 2023;110:105-119.
5. Hengel H, Pellerin D, Wilke C, et al. As Frequent as Polyglutamine Spinocerebellar Ataxias: SCA27B in a Large German Autosomal Dominant Ataxia Cohort. *Mov Disord* 2023;38:1557-1558.
6. Wilke C, Pellerin D, Mengel D, et al. GAA-FGF14 ataxia (SCA27B): phenotypic profile, natural history progression and 4-aminopyridine treatment response. *Brain* 2023.
7. Bonnet C, Pellerin D, Roth V, et al. Optimized testing strategy for the diagnosis of GAA-FGF14 ataxia/spinocerebellar ataxia 27B. *Scientific reports* 2023;13:9737.
8. Bonnet C, Pellerin D, Roth V, et al. Optimized testing strategy for the diagnosis of GAA-FGF14 ataxia. *medRxiv* 2023:2023.2002.2002.23285206.
9. Salonen O, Autti T, Raininko R, Ylikoski A, Erkinjuntti T. MRI of the brain in neurologically healthy middle-aged and elderly individuals. *Neuroradiology* 1997;39:537-545.
10. Metwally MI, Basha MAA, AbdelHamid GA, et al. Neuroanatomical MRI study: reference values for the measurements of brainstem, cerebellar vermis, and peduncles. *Br J Radiol* 2021;94:20201353.
11. Gupta T, Singh B, Kapoor K, Gupta M, Kochar S. Corpus callosum morphometry: comparison of fresh brain, preserved brain and magnetic resonance imaging values. *Anat Sci Int* 2008;83:162-168.
12. Schmidt R, Schmidt H, Haybaeck J, et al. Heterogeneity in age-related white matter changes. *Acta neuropathologica* 2011;122:171-185.
13. Manjon JV, Coupe P. volBrain: An Online MRI Brain Volumetry System. *Front Neuroinform* 2016;10:30.
14. Park MT, Pipitone J, Baer LH, et al. Derivation of high-resolution MRI atlases of the human cerebellum at 3T and segmentation using multiple automatically generated templates. *Neuroimage* 2014;95:217-231.
15. Iruzubieta P, Pellerin D, Bergareche A, et al. Frequency and phenotypic spectrum of spinocerebellar ataxia 27B and other genetic ataxias in a Spanish cohort of late-onset cerebellar ataxia. *Eur J Neurol* 2023.
16. Guerrini L, Lolli F, Ginestroni A, et al. Brainstem neurodegeneration correlates with clinical dysfunction in SCA1 but not in SCA2. A quantitative volumetric, diffusion and proton spectroscopy MR study. *Brain* 2004;127:1785-1795.
17. Velazquez-Perez LC, Rodriguez-Labrada R, Fernandez-Ruiz J. Spinocerebellar Ataxia Type 2: Clinicogenetic Aspects, Mechanistic Insights, and Management Approaches. *Front Neurol* 2017;8:472.
18. Eichler L, Bellenberg B, Hahn HK, Koster O, Schols L, Lukas C. Quantitative assessment of brain stem and cerebellar atrophy in spinocerebellar ataxia types 3 and 6: impact on clinical status. *AJNR American journal of neuroradiology* 2011;32:890-897.
19. Lebre AS, Brice A. Spinocerebellar ataxia 7 (SCA7). *Cytogenet Genome Res* 2003;100:154-163.
20. Lilja A, Hamalainen P, Kaitaranta E, Rinne R. Cognitive impairment in spinocerebellar ataxia type 8. *Journal of the neurological sciences* 2005;237:31-38.

21. Loy CT, Sweeney MG, Davis MB, et al. Spinocerebellar ataxia type 17: extension of phenotype with putaminal rim hyperintensity on magnetic resonance imaging. *Mov Disord* 2005;20:1521-1523.
22. Vemuri P, Castillo AM, Thostenson KB, et al. Imaging biomarkers for early multiple system atrophy. *Parkinsonism Relat Disord* 2022;103:60-68.
23. Pierrot-Deseilligny C, Milea D. Vertical nystagmus: clinical facts and hypotheses. *Brain* 2005;128:1237-1246.
24. Blazquez PM, Pastor AM. Cerebellar Control of Eye Movements. In: Manto MU, Gruol DL, Schmahmann JD, Koibuchi N, Sillitoe RV, eds. *Handbook of the Cerebellum and Cerebellar Disorders*. Cham: Springer International Publishing, 2022: 1301-1318.
25. Wirth T, Clément G, Delvallée C, et al. Natural History and Phenotypic Spectrum of GAA-FGF14 Sporadic Late-Onset Cerebellar Ataxia (SCA27B). *Mov Disord* 2023.
26. Novis LE, Frezatti RS, Pellerin D, et al. Frequency of GAA-FGF14 Ataxia in a Large Cohort of Brazilian Patients With Unsolved Adult-Onset Cerebellar Ataxia. *Neurol Genet* 2023;9:e200094.
27. Pellerin D, Heindl F, Wilke C, et al. Intronic FGF14 GAA repeat expansions are a common cause of downbeat nystagmus syndromes: frequency, phenotypic profile, and 4-aminopyridine treatment response. *medRxiv* 2023.
28. Grodd W, Hulsman E, Lotze M, Wildgruber D, Erb M. Sensorimotor mapping of the human cerebellum: fMRI evidence of somatotopic organization. *Hum Brain Mapp* 2001;13:55-73.
29. Schmahmann JD, Macmore J, Vangel M. Cerebellar stroke without motor deficit: clinical evidence for motor and non-motor domains within the human cerebellum. *Neuroscience* 2009;162:852-861.
30. Timmann D, Brandauer B, Hermsdorfer J, et al. Lesion-symptom mapping of the human cerebellum. *Cerebellum* 2008;7:602-606.
31. Mascalchi M, Diciotti S, Giannelli M, et al. Progression of brain atrophy in spinocerebellar ataxia type 2: a longitudinal tensor-based morphometry study. *PLoS One* 2014;9:e89410.
32. Stezin A, Bhardwaj S, Khokhar S, et al. In vivo microstructural white matter changes in early spinocerebellar ataxia 2. *Acta Neurol Scand* 2021;143:326-332.
33. Selvadurai LP, Georgiou-Karistianis N, Shishegar R, et al. Longitudinal structural brain changes in Friedreich ataxia depend on disease severity: the IMAGE-FRDA study. *J Neurol* 2021;268:4178-4189.
34. Adanyeguh IM, Joers JM, Deelchand DK, et al. Brain MRI detects early-stage alterations and disease progression in Friedreich ataxia. *Brain Commun* 2023;5:fcad196.
35. Infante J, Serrano-Cárdenas KM, Corral-Juan M, et al. POLR3A-related spastic ataxia: new mutations and a look into the phenotype. *Journal of Neurology* 2020;267:324-330.
36. Minnerop M, Kurzwelly D, Wagner H, et al. Hypomorphic mutations in POLR3A are a frequent cause of sporadic and recessive spastic ataxia. *Brain* 2017;140:1561-1578.
37. Kim M, Ahn JH, Cho Y, Kim JS, Youn J, Cho JW. Differential value of brain magnetic resonance imaging in multiple system atrophy cerebellar phenotype and spinocerebellar ataxias. *Scientific reports* 2019;9:17329.
38. Burk K, Buhring U, Schulz JB, Zuhlke C, Hellenbroich Y, Dichgans J. Clinical and magnetic resonance imaging characteristics of sporadic cerebellar ataxia. *Arch Neurol* 2005;62:981-985.
39. Ouyang R, Wan L, Pellerin D, et al. The genetic landscape and phenotypic spectrum of GAA-FGF14 ataxia in China: a large cohort study. *eBioMedicine* 2024;102:105077.

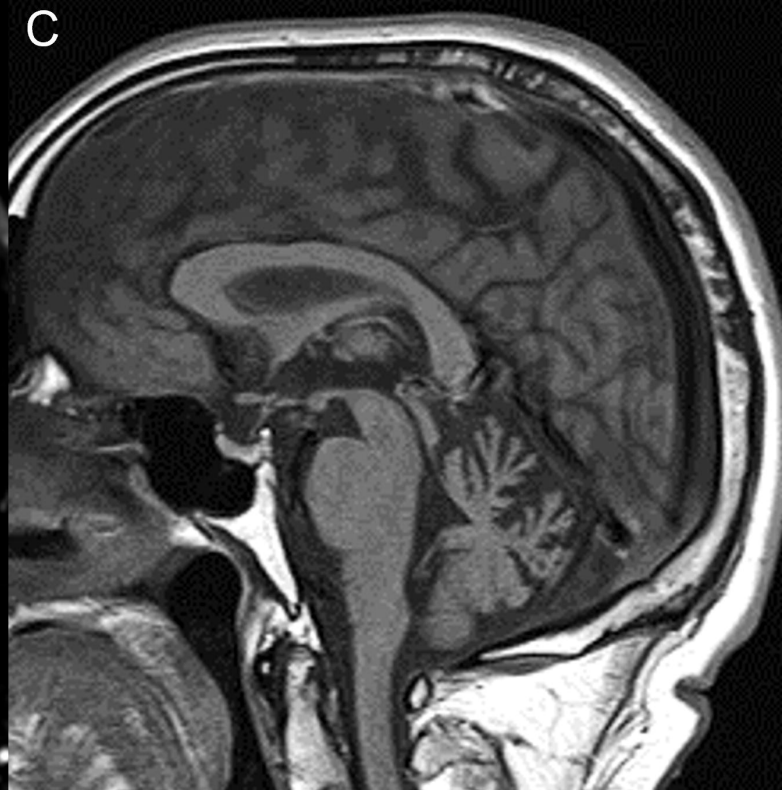
A



B



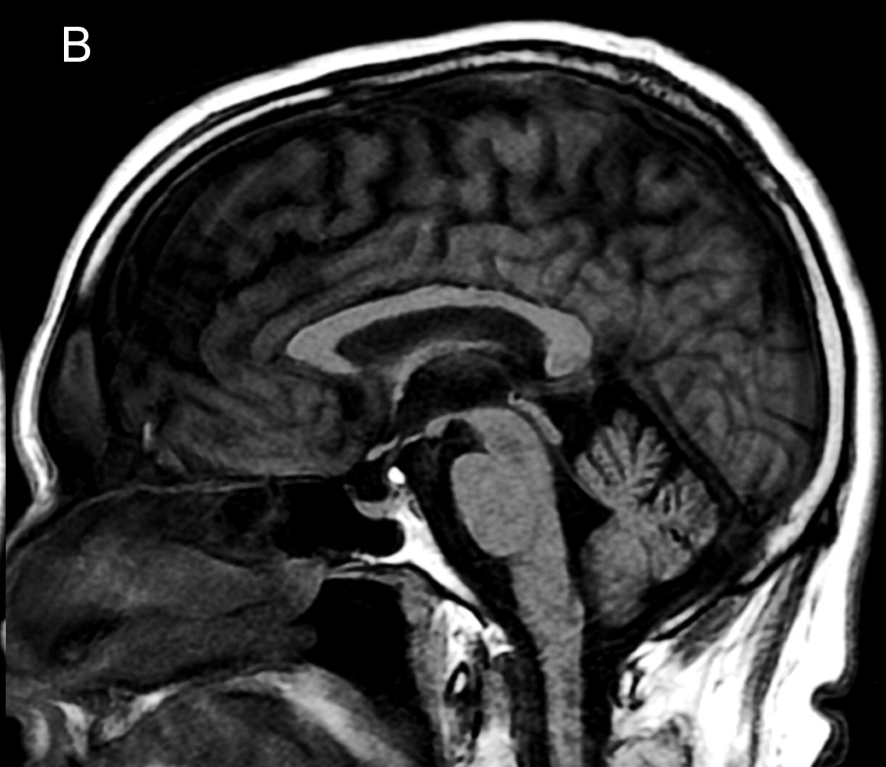
C



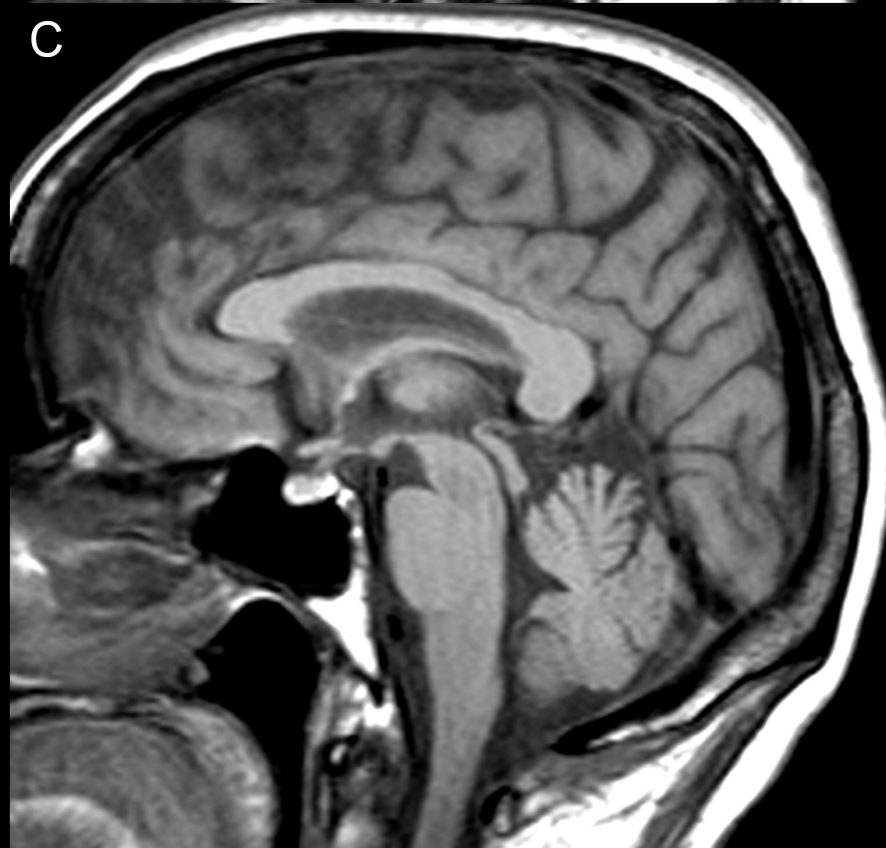
A



B



C



D



